Journal of Catalysis **211,** 33–41 (2002)
doi:10.1006/jcat.2002.3727

The Working State of the Barium Promoter in Ammonia Synthesis over an Active-Carbon-Supported Ruthenium Catalyst Using Barium Nitrate as the Promoter Precursor

Hai Sheng Zeng, Koji Inazu, and Ken-ichi Aika[1]

Department of Environmental Chemistry and Engineering, Interdisciplinary Graduate School of Science and Engineering,
Tokyo Institute of Technology, 4259 Nagatsuta, Midori-ku, Yokohama 226-8502, Japan

Received August 27, 2001; revised June 17, 2002; accepted June 27, 2002

Barium-promoted Ru/HTAC (hydrogen-treated active carbon) is reported to be a promising ammonia catalyst. However, deactivation and regeneration have been observed under some conditions. In this study, the activity change of this catalyst was studied in detail. The effects of the reaction temperature, $Ba(NO_3)_2$ decomposition temperature, and the water vapor pressure on the ammonia-synthesis activity were investigated to elucidate the cause. It was found that the promoter components under reaction conditions were BaO and $Ba(OH)_2$, of which the molar ratio varied with the temperature and water vapor pressure, obeying the reversible reaction $BaO + H_2O = Ba(OH)_2$. It was concluded that the activity was changed reversibly depending on the chemical form, BaO or $Ba(OH)_2$. The stronger promoting effect of BaO vs. $Ba(OH)_2$ was attributed to its stronger electron donation to Ru. The activity drop at 588 K of the sample activated at 823 K was concluded to be due to the decrease of the BaO portion resulting from the contained water vapor (10 Pa is the threshold at 648 K). At high temperature, deactivation can not occur because of the thermodynamic equilibrium of $BaO/Ba(OH)_2$. For alkali metals, their hydroxides (CsOH or KOH) are not considered to turn to the active-oxide phase under the usual ammonia-synthesis conditions.

Key Words: **ammonia synthesis; BaO and $Ba(OH)_2$ promoter; active-carbon-supported ruthenium catalyst; active-promoter phase; deactivation with water vapor; ruthenium catalysts.**

1. INTRODUCTION

Ruthenium-based catalysts have been studied for many years (1, 2) and industrialized by the BP group (3, 4) but there are still challenging problems to be solved for ruthenium catalysts: active center, promoter, kinetics, etc. These problems are related to the fundamental principles for metal catalysis and also are the keys for further development of industrial ruthenium catalysts.

So far the electronic donation theory has been widely applied to explain ruthenium catalysis. A surface-metal atom is supposed to donate electrons through the d orbital to the antibonding orbital of N_2, which substantially weakens the N≡N triple bond and makes the N_2-dissociation reaction easier (1, 2). When it donates more electrons and has a stronger bond with ruthenium surface atoms, the lifetime of the adsorbed dinitrogen molecule is considered to be longer. This may cause a high sticking coefficient of dissociative adsorption (electronic effect). In the case of Ru catalysts, therefore, promoters and supports facilitating electron donation are favored (5–14). The promoting factor is inversely proportional to the electron negativity of the promoter oxide or hydroxide (1, 15). As promoter precursors, nitrates, of alkali metals and alkaline earth metals such as K, Cs, Ba, etc., which turn to oxides or hydroxides, are selected in most cases (7, 16–25). On the other hand, dinitrogen must be bound to two ruthenium atoms finally, and thus the surface ruthenium structure must have some role (structural effect).

Recent remarkable advances have come from surface scientific approaches or research using new instruments. Dahl *et al.* proved that the step site (or B5 site) of the Ru surface is the active center of dinitrogen dissociation (26). The ammonia synthesis, whose rate-determining step is dissociative adsorption of dinitrogen, is well known to be the structure-sensitive reaction. Although this was proved for an iron single-crystal surface, whose (111) surface is extraordinarily more active than other surfaces (27), it was also proved for the ruthenium surface (26). Hinrichsen *et al.* also proposed that the active center is just a part of the ruthenium cluster which is connected to the support MgO (28, 29). A microkinetic study rendered a bridge between the surface science condition and the practical condition (28, 30). The method seems to be successful in extending the kinetic parameter obtained on a single-crystal surface for expressing the rate data on the supported catalysts at high pressure.

Despite these enormous efforts, the promoter problem still seems unsolved. Industrial ruthenium catalysts could not be prepared without the promoter, which accelerates

---

[1] To whom correspondence should be addressed. Fax: +81-45-924-5441. E-mail: kenaika@chemenv.titech.ac.jp.

0021-9517/02 $35.00

the reaction tremendously and may change the kinetics (1, 2). The following simple questions arise about the promoter's role:

1. Does the promoter molecule help creating the active structure of the ruthenium surface (such as the B5 site) through reconstruction (29, 31)? This kind of idea has been proposed for the iron catalyst (27, 32).
2. Does the promoter only donate electrons to normal Ru surfaces, weakening the N–N bond and accelerating dinitrogen dissociation (5–14)?
3. Does the promoter further help the dissociation at the special site (such as the B5 site) by the combination of the structural effect and electronic effect (33)?

If these guiding principles about promoter action are clarified, the accumulated work can be explained and better catalysts can be further developed.

Another recent development is the use of barium as a promoter. $Ba(NO_3)_2$ has been proven to be an excellent promoter precursor for the Ru/active-carbon (AC) catalyst for ammonia synthesis (17, 23, 24, 34, 35). Carbon-supported Ru catalysts with promoters have been reported to be active for ammonia synthesis and one kind with graphitic carbon has been industrialized as a second-generation catalyst (3, 4). Active carbon becomes much more effective when treated with hydrogen at 1173 K for this system (34, 36).

Ba-doped ruthenium has been found to be more active than Cs-doped ruthenium for zeolite support (37), MgO support (29), and carbon support (38). The interaction between BaO and the Ru surface has been studied in atomic scale (31). Ba-doped Ru must be quite important for industry. Our groups also studied Ba-doped Ru catalysts for many years (24, 34). Usually these are not as active as Cs-doped catalysts. Moreover, Ba-doped Ru is unstable, sometimes deactivates, and can be regenerated. To clarify the reason for this during the study we suspected that the key to the stability would be the chemical form of the Ba promoter or the interaction of Ru with the Ba promoter. This must be studied under the reaction condition.

There are not many studies about the promoter for the Ru catalyst in the working state. Most of the literature thus far discusses the role of the support or promoter as it is, but does not discuss the *in situ* state (23, 25, 39–41). After hydrogen treatment or under ammonia-synthesis conditions, $Ba(NO_3)_2$ was proposed to be decomposed to form hydroxide or oxide, although the exact chemical state was not identified (24, 34). Some studies on the state of the promoter were made for $CsNO_3$ and KNO_3 (8, 15, 16, 25, 41). What is the chemical state of the promoter under the ammonia-synthesis reaction? Which phase of the Ba promoter is more active for the Ru/AC catalyst, the oxide form or the hydroxide form? How does the promoter locate on the catalyst morphologically? These problems have not been sufficiently studied so far. There was also an unsolved problem wherein activity dropped during the run of ammonia synthesis and could be recovered by high-temperature treatment for the $Ba(NO_3)_2$-promoted Ru/AC catalyst (42). Water- or oxygen-containing molecules, e.g., O_2, CO, CO_2, are generally known as poisons for the ammonia-synthesis catalyst. The poisoning is either reversible or irreversible, depending on the catalysts or the working conditions. This problem is important for commercial operations.

In this study, the active form of a promoter derived from the $Ba(NO_3)_2$ precursor over the Ru/AC catalyst was studied in detail for the first time. The effect of moisture (water vapor) contained in the synthesis gas was studied and a thermogravimetric analysis (TGA) was also done. Combined with the obtained results, interpretation of the promoter effect for the Ru/AC catalyst was further discussed.

2. EXPERIMENTAL

2.1. *Catalyst Preparation and Activation*

First, temperature-programmed treatment of raw AC (bead-shaped, average diameter around 0.7 mm, made of pitch, Kureha Chemical Industries) with H_2 (20 ml/min) was carried out at 1173 K for 90 h to remove the electron-withdrawing impurities such as =S, =NH, –COOH, –CHO, halogen, etc., which can be poisonous for ammonia synthesis (36, 43). The hydrogen-treated AC was used as support and is indicated as HTAC hereafter. The properties of HTAC (surface area, elemental analysis, etc.) have been reported (36, 43). HTAC was impregnated with $RuCl_3$ (Ru : HTAC = 5 : 100 wt/wt) in acetone. After drying at 373 K the obtained $5RuCl_3$/HTAC was treated with H_2 to remove the poisonous chlorine and to form metallic Ru on HTAC (i.e., 5Ru/HTAC) at a fixed temperature of 723 K for 24 h, conditions that were suggested to be optimal (44). Finally, 5Ru/HTAC was impregnated with $Ba(NO_3)_2$ (promoter precursor) in water with an equivalent molar ratio of Ba to Ru. The dried sample was labeled $1Ba(NO_3)_2$–5Ru/HTAC.

2.2. *Ammonia Synthesis and Activity Measurement*

The ammonia-synthesis reaction was performed in a computer-controlled flow system with synthesis gas $N_2 + 3H_2$ (60 ml/min, 1 atm) over 0.2-g catalyst ($SV = 18000\ h^{-1}$) (Fig. 1). Before an activity test run, the catalyst was treated with H_2 (50 ml/min) for 3 h to decompose the $Ba(NO_3)_2$ precursor or to activate the catalyst (nitrate-decomposition process). The reaction temperature (R-x K) and the nitrate decomposition temperature (D-x K) vary from 588 to 823 K, respectively. The ammonia-synthesis rate was determined by measuring the decrease rate of electric conductivity of the 200-ml 0.00216 N H_2SO_4 solution that absorbed the produced NH_3.

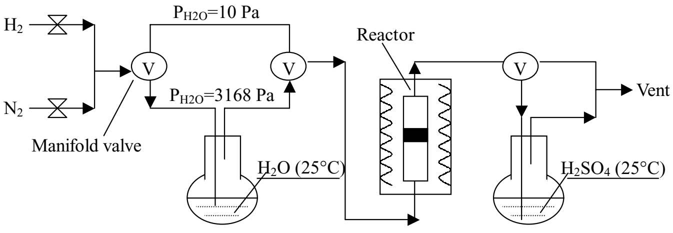

FIG. 1. Experimental apparatus carrying water vapor with synthesis gas into the reactor. 10 Pa of water impurity is assumed to come from the commercial gas ($N_2 + 3H_2$) cylinder while 3170 Pa of saturated water vapor comes through a bubbler.

2.3. *Water Vapor Feeding Test*

Prior to an activity test run, water vapor was fed by switching the synthesis gas line to a water bubbler at 298 K for 5 min (Fig. 1). In this case the synthesis gas carries the saturated water vapor at 3170 Pa. After a 5-min water vapor feeding, the synthesis-gas flow was switched back to the original route. The amount of a 1-min water vapor feeding would make $H_2O : Ba : Ru = 1 : 1 : 1$ in a molar ratio on the 0.2-g $1Ba(NO_3)_2$–5Ru/HTAC catalyst.

2.4. *TGA*

TGA (Seiko SSC/5200) was carried out during the nitrate-decomposition process of pure $Ba(NO_3)_2$ (about 50 mg) with a temperature increment rate of 6 K/min under H_2 (80 ml/min) at ambient atmosphere.

3. RESULTS

3.1. *Activation, Deactivation, and Reactivation of the Catalyst*

Figure 2A indicates the activity change with the hydrogen treatment. At low treatment temperature, because the decomposition of the promoter precursor $Ba(NO_3)_2$ is not complete, the activity is low. After increasing the treatment temperature to 823 K, the decomposition of $Ba(NO_3)_2$ is completed and the active promoter component is formed, hence leading to as much as twice the activity.

As shown in Fig. 2B, the run of time onstream, the activity decreased gradually from 1250 to 250 μmol/h/g in 10 h. Apparently the catalyst was drastically deactivated. It is interesting to find that the deactivated catalyst was reactivated by hydrogen treatment, as shown in Fig. 2C. The recovered activity strongly depends on the treatment temperature. When the treatment temperature was increased to 823 K again, the highest activity was recovered. However, the regenerated catalyst deactivated gradually again in 10 h (Fig. 2D).

Some change must have occurred repeatedly on the catalyst following the change of temperature again and again. (A similar phenomenon is seen in the literature (45) where PdO is said to be transformed to Pd above 1123 K, while the reverse transformation occurs below 953 K under the air.) Since the activation–deactivation is reversible and depends on the treatment temperature, the factor controlling the activity should be also reversible with the treatment temperature. According to the bulk thermodynamic calculation (listed in a later section), the Ru particle must always be metallic under a hydrogen stream or reactant gas ($N_2 + 3H_2$) stream at these treatment temperatures. The suspicion that the change of the Ru particle size is the cause is also excluded because there is no reason for the Ru particle size to be decreased with temperature increase. The most possible cause must be the variation of the promoter components or states. It was concluded that the precursor $Ba(NO_3)_2$ is decomposed to BaO or $Ba(OH)_2$ during the hydrogen treatment on Ru/HTAC (36, 44). BaO and $Ba(OH)_2$ can be changeable with the temperature and water vapor; $BaO + H_2O = Ba(OH)_2$ with $\Delta H^0_{298} = -34.9$ kcal/mol. Here, the change of the ratio of BaO to $Ba(OH)_2$ is tentatively presumed to be the cause for the phenomena of activation, deactivation, and reactivation of the catalyst. This presumption is confirmed reasonably by the following experiments.

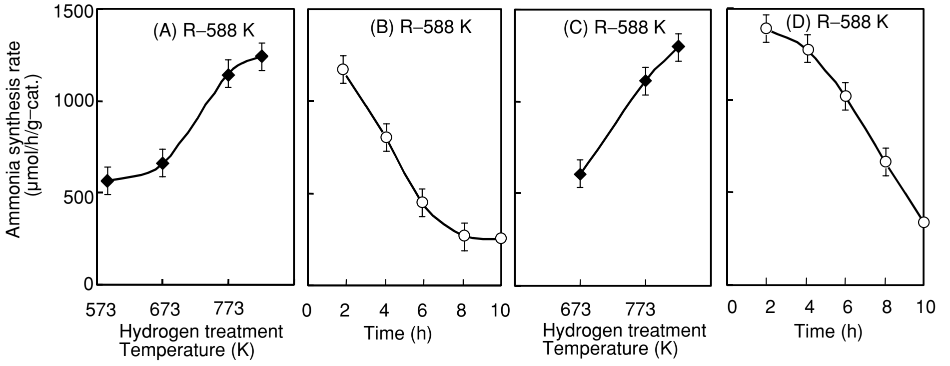

FIG. 2. Effect of hydrogen treatment temperature on the catalytic activity (A, C) and time onstream of the activity (B, D), respectively. Four runs were carried out continuously on the same catalyst. Activity was measured at 588 K under 1 atm of $N_2 + 3H_2$ with SV of 18,000 h^{-1} over 1Ba–5Ru/HTAC.

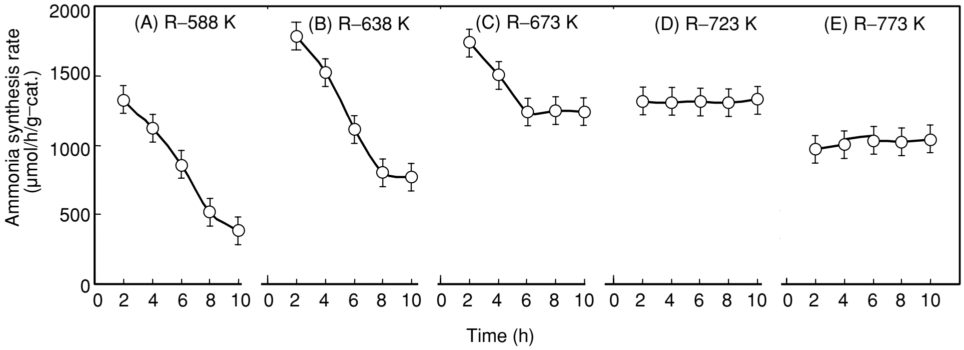

FIG. 3. Effect of reaction temperature on the deactivation profile. Prior to each run the catalyst was treated with hydrogen at 823 K for 3 h. Activity was measured at 588, 638, 673, 723, and 773 K under 1 atm of $N_2 + 3H_2$ with SV of 18,000 h^{-1} over 1Ba–5Ru/HTAC.

3.2. The Reaction Temperature and Activity Change

To verify the preceding presumption, the reaction temperature was changed and the activity change was observed (Fig. 3). The same activity change was observed at the reaction temperature of 588 K after treating at 823 K (Fig. 3A) as in the case of Fig. 2A. The activity after 10 h was 22% of the initial activity. After increasing the reaction temperature to 683 K (Fig. 3B), even though the activity was decreased at a similar rate first, the decrease of activity ceased at 8 h, keeping 43% of the initial activity. With a further increase of the reaction temperature to 673 K (Fig. 3C), after an initial drop of the activity it reached a stable zone at 6 h, keeping 75% of the initial activity. For reaction temperatures of 723 and 773 K (Figs. 3D and 3E), the initial activities were maintained the entire time.

These results can be explained by the preceding presumption in terms of the reversible change of the active-promoter components. After the treatment at 823 K a larger amount of active-promoter component is produced. If the reaction temperature is low (e.g., 588 K), the thus-produced active-promoter component could not be maintained, but decreased with time onstream; consequently, the activity decreased. When the reaction temperature is high (e.g., 638, 673 K), the temperature gap between the treatment (823 K) and the reaction is not much. Under these circumstances, after the initial small drop, the active component must be kept high during the ammonia-synthesis process. For the case of the extremely high reaction temperatures of 723 and 773 K, since the activity did not drop, it is probable that the active-promoter phase was sufficiently maintained. But on the other hand, the activity level itself is low because of the thermodynamic equilibrium limit of ammonia syntheses. Different runs were tested to check the reproducibility in the activity performances, although the catalyst deactivation speed was different probably due to the different level of water impurity from the source. The activation and reactivation profiles were similar and repeatable.

3.3. Effect of Water Vapor

Activity change was explained by the change of the promoter-phase BaO/Ba$(OH)_2$, which depended on the temperature. According to the presumption, besides the temperature, the water vapor pressure must be another factor influencing the active-promoter component phase of BaO/Ba$(OH)_2$. In the last section, the water vapor (i.e., moisture) was assumed to come from the commercial gas cylinder (Fig. 1). Water vapor pressure of 10 Pa is assumed in this case, and is discussed later. The water content in each cylinder may differ. To verify the preceding presumptions, some level of water vapor pressure was introduced to the catalyst.

In these runs the activity was rather stable, as shown in Fig. 4A, at 588 K in a short range of time (0–4 h). In this case the water impurity level must be lower than the case in Fig. 1. Therefore, under the run of a short time onstream, the activity change due to added water vapor can be checked. After this run (Fig. 4A), water vapor of 3170 Pa was fed for 5 min and the activity was measured (Fig. 4B). After exposure with water vapor, the activity promptly decreased to

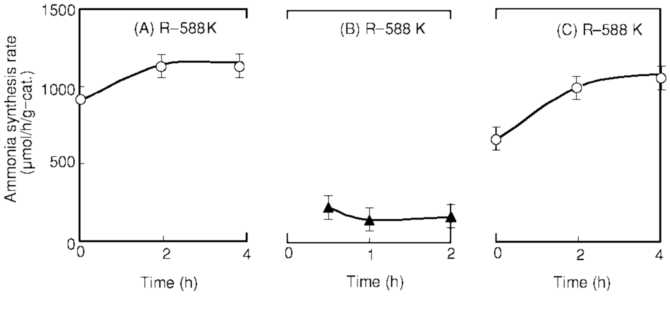

FIG. 4. Effect of water vapor feeding on activity at 588 K. Prior to runs A and C, the catalyst was treated with hydrogen at 823 K for 3 h. Prior to run B, water vapor of 3170 Pa was fed for 5 min. Activity was measured under 1 atm of $N_2 + 3H_2$ at 588 K with SV of 18,000 h^{-1} over 1Ba–5Ru/HTAC.

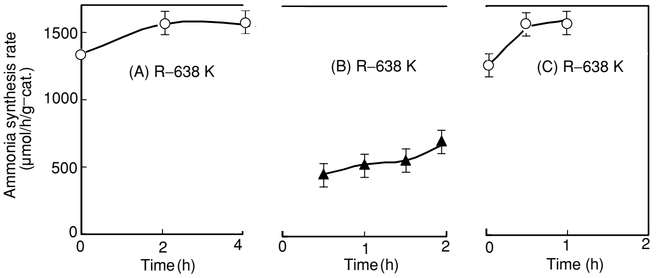

FIG. 5. Effect of water vapor feeding on activity at 638 K. Treatment conditions are the same as in Fig. 4.

13% of the initial activity (Fig. 4B). By hydrogen treatment at 823 K, the activity was completely recovered (Fig. 4C) to the same level as in Fig. 4A.

Similar activity change was also observed as per Figs. 5, 6, and 7 at reaction temperatures of 638, 673, and 723 K, respectively. The only difference with these results is a slight increase of activity after the initial drop (Figs. 5B, 6B, and 7B). After the hydrogen treatment at 823 K, similarly, the lost activity was completely recovered (Fig. 5C).

The recovery was 60% at 2 h of time onstream under the reaction temperature of 673 K (Fig. 6B). However, it was about 100% under the reaction temperature of 723 K (Fig. 7B). The catalytic activity was completely regenerated without the hydrogen treatment at 823 K.

In brief, both under the assumed low water vapor pressure of 10 Pa (or low) and under the presence of the actual high water vapor pressure of 3170 Pa for a short time, the tendency of activity change was almost identical. The latter gave evidence that supported the presumption to be reasonable as follows.

After the water vapor feeding (3170 Pa) for 5 min, the presence of a large amount of H_2O turned the active-promoter component BaO to $Ba(OH)_2$ and consequently the amount of BaO was decreased, promptly decreasing the activity. After a 5-min water vapor feeding, gradually the superfluous amount of H_2O was carried away from the reactor by the synthesis gas and finally the circumstance water vapor was kept to the 10 Pa (or lower in these runs) level in the synthesis gas. Then, a part of $Ba(OH)_2$ started to decompose to form BaO. Thermodynamically, the portion of regenerated BaO is large at a high temperature. As a result, the recovery of catalytic activity is increased with the increase of reaction temperature from 588 to 723 K. After a run at low reaction temperature, high-temperature treatment is needed to regenerate BaO and recover the catalytic activity.

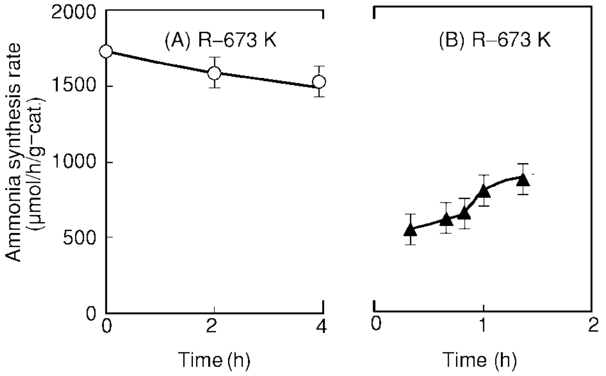

FIG. 6. Effect of water vapor feeding on activity at 673 K. Prior to run A, the catalyst was treated with hydrogen at 823 K for 3 h. Prior to run B, water vapor of 3170 Pa was fed for 5 min. Activity was measured under 1 atm of $N_2 + 3H_2$ at 673 K with $SV = 18000\ h^{-1}$ over 1Ba–5Ru/HTAC.

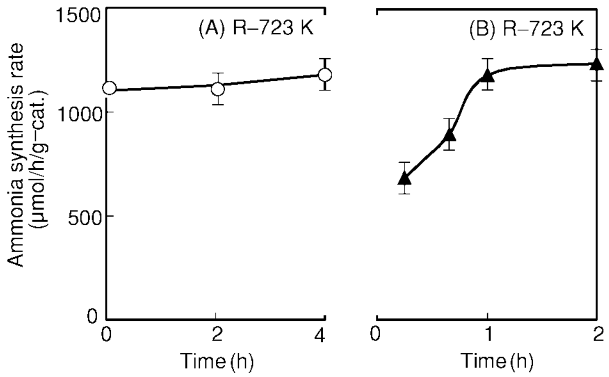

FIG. 7. Effect of water vapor feeding on activity at 723 K. Treatment conditions are the same as in Fig. 6.

3.4. *TGA of Hydrogenolysis Process of $Ba(NO_3)_2$*

The TG-MS analysis of the hydrogenolysis process of the $1Ba(NO_3)_2$–5Ru/HTAC catalyst was done (43). It has been reported that the decomposition of $Ba(NO_3)_2$ starts at about 553 K. At temperature above 748 K of H_2 treatment, the methanation of carbon support occurs, which surely interferes with the signal of weight change due to the interconversion between BaO and $Ba(OH)_2$. To verify the preceding presumption further, hydrogen treatment of "pure" $Ba(NO_3)_2$ was carried out in the H_2 stream through TGA and the corresponding results are shown in Fig. 8.

From the differential thermogravimetry (DTG) curve (Fig. 8B), it is understood that a small amount of coordinated water is desorbed at about 423 K, whereas the decomposition of $Ba(NO_3)_2$ starts at 693 K, which is much higher than that for the $1Ba(NO_3)_2$–5Ru/HTAC catalyst in the H_2 stream. This means that the dissociated hydrogen atom on the Ru surface promotes the decomposition of $Ba(NO_3)_2(Ba(NO_3)_2 + 8H_2 \rightarrow BaO + 5H_2O + 2NH_3)$ (43). After maintaining the reaction at 933 K for about 30 min, the decomposition of $Ba(NO_3)_2$ is completed $Ba(NO_3)_2 \rightarrow BaO + NO_2 + NO_3$ (Fig. 8A, point b). DTG is near 0 μg/min (Fig. 8B) and TG reaches a plateau even though the treatment time is extended.

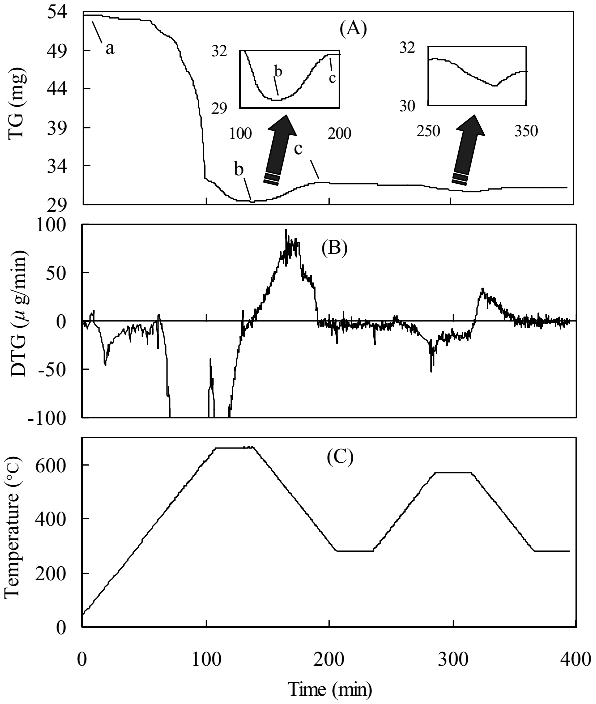

FIG. 8. TGA profile of the hydrogen treatment of $Ba(NO_3)_2$ with amplified patterns. Treatment conditions: H_2, 80 ml/min, 1 atm, 6 K/min.

Hereafter, the temperature was decreased to 553 K at a stable decreasing rate. A positive DTG peak was observed. Correspondingly, the TG of the sample increased from 29.42 mg (Fig. 8A, point b) to 31.82 mg (point c) (Table 1). It can be concluded that, with the decrease of circumstance temperature, the BaO once produced at the high temperature reacts with H_2O (moisture) to form $Ba(OH)_2$.

To further confirm this phenomenon, the increase–decrease temperature sequence was repeated (200–400 min) and similar results were obtained. Since the highest progressive temperature was 833 K, which was lower than the previous temperature of 933 K, the DTG peaks and TG amounts changed on a small scale.

A calculation was done and is summarized in Table 1. It can be found that at 933 K of point b (Fig. 8A), almost all the Ba derivatives were in the BaO form ($Ba(OH)_2 : BaO = 0 : 1$ mol/mol). When the temperature was decreased to 643 K (Fig. 8A, point c), the molar ratio of $Ba(OH)_2 : BaO$ was changed to approximately 7 : 3. The moisture contained in the synthesis gas from the commercial gas cylinder was estimated to be 745 ppm in this experiment. The calculated moisture concentration seems to be much higher than that of the run in Fig. 2. The obtained value might include the contribution from water adsorbed on the wall of TG instruments. The TGA results confirm the presumption that the Ba derivatives can reversibly be changed with temperature obeying the equilibrium reaction: $BaO + H_2O = Ba(OH)_2$ with $\Delta H^0_{298} = -34.9$ kcal/mol.

TABLE 1

Variation of TG (Fig. 8) and Calculated Components Molar Ratio during Hydrogen Treatment of $Ba(NO_3)_2$ (0.2045 mol)

Point in Fig. 8	Time (min)	Temperature (K)	TG (mg)	$Ba(NO_3)_2 : Ba(OH)_2 : BaO$[a] (mol/mol/mol)
a	0	333	53.44	1 : 0 : 0
b	140	933	29.42	0 : 0 : 1
c	190	643	31.82	0 : 0.7 : 0.3

[a] Calculation error is estimated to be 6%.

4. DISCUSSION

4.1. *Working State of Promoter and Catalytic Activity*

All of these results in activity and characterization support the presumption that promoter components vary with the treatment temperatures and water pressures obeying the reversible reaction between BaO and $Ba(OH)_2$. Table 2 depicts the theoretical evaluation from the reaction equilibrium. It shows that the treatment temperature greatly changes the promoter phase depending on the water vapor pressure. And hence it controls the catalytic activity.

Prior to an activity test, the catalyst was treated, for example at 823 K, where the equilibrium pressure of water vapor was 639 Pa. If the synthesis gas contains 10 Pa of water vapor, most of the $Ba(OH)_2$ decomposes to BaO and H_2O. The produced 639 Pa of H_2O is carried away with the flow of treatment gas and the BaO-promoted Ru/HTAC is active in the ammonia synthesis at 588 K. However, the equilibrium water vapor pressure at 588 K is about 4 Pa, which is lower than the 10 Pa of impure water vapor pressure. Here, BaO reacts with H_2O to form $Ba(OH)_2$, resulting in a gradual decrease of the initial activity (Fig. 2B). This can be reproduced (Figs. 2C and 2D) because the process is reversible. Since $Ba(OH)_2$ is the major phase at 638 K (Table 2), the activity drops (Fig. 3B). However, two phases may exist at 673 K (Table 2), where the activity drops to some extent (Fig. 3C). The activity is stable at 723 and 773 K because the major phase is BaO (Table 2).

When the water vapor pressure is high (3170 Pa), $Ba(OH)_2$ is the major phase below 673 K (Table 2), resulting in the activity drop at 588 K (Fig. 4), 638 K (Fig. 5), and 673 K (Fig. 6). At 723 K, two phases may coexist (Table 2) where the activity drop is small (Fig. 7).

Our groups have reported the function of the Ba-doped Ru catalyst for many years (24, 34). Usually these are not as active as Cs-doped catalysts, contrary to the finding in other works (29, 37, 38). Moreover, our Ba-doped Ru was unstable, sometimes deactivated, but able to be regenerated. All these phenomena can be explained by the aforementioned theory: interconversion between BaO and $Ba(OH)_2$, depending on the temperature and water vapor pressure of

TABLE 2

Calculated Water Vapor Pressure of Reaction Equilibrium (49); $BaO + H_2O = Ba(OH)_2$ with $\Delta H^0_{298} = -34.9$ kcal/mol; and Major Phase of Promoter under Different Temperature and Water Vapor Pressure

Temperature (K)	573	623	673	773	873	973
Equilibrium P_{H_2O} (Pa)	0.5	4	23	639	7340	47390
Run under $P_{H_2O} = 10$ Pa	$Ba(OH)_2$	$Ba(OH)_2$	BaO	BaO	BaO	BaO
Run under $P_{H_2O} = 3170$ Pa	$Ba(OH)_2$	$Ba(OH)_2$	$Ba(OH)_2$	$Ba(OH)_2$	BaO	BaO

the system. Since it is hard to control or to measure the water pressure of the ppm level in the line, the activity at a rather low temperature, such as 588 K, can be deactivated during the measurements.

This conclusion is strongly supported by the principle that the promoting effect of promoters on the Ru catalyst is inversely proportional to the compound electronegativity (1, 15). Because BaO has a lower electronegativity (1.77) than $Ba(OH)_2$ (2.17) (46), BaO donates more electrons to the Ru surface, resulting in more activity for ammonia synthesis than $Ba(OH)_2$. The authors do not claim that the BaO phase is the only active-promoter state. A BaO monolayer on the Ru surface can be the active state of the promoter, as suggested in a recent report (31). The interconversion of $BaO/Ba(OH)_2$ can occur on the Ru surface although the equilibrium constant might be somewhat different in the layered form.

As a cause of water inhibition, metal-surface oxidation might be considered, such as in the case of an iron catalyst. However, the equilibrium constant of reaction $Ru + 2H_2O = RuO_2 + 2H_2$ is about 6.76×10^{-12} at 773 K, whereas it is 6.31×10^{-3} for reaction $BaO + H_2O = Ba(OH)_2$ (Table 2). Therefore, oxidation of the active site (Ru surface atom) can be excluded in the case of ruthenium.

4.2. *Comparison of Alkali-Metal and Alkaline-Earth-Metal Promoters*

The preceding finding is considered to be instructive for understanding other alkali-metal promoters such as Cs, K, etc., on Ru/AC catalysts. It has been claimed that the $CsNO_3$-promoted Ru/AC catalyst had a stable activity even under a low reaction temperature (34, 42). This phenomenon is much different from that of the Ba-promoted Ru/AC catalyst in this study. A possible reason is that the reaction $Cs_2O + H_2O = 2CsOH$ has a much higher equilibrium constant (K_p) than the $Ba(OH)_2$ case. Namely, under normal reaction conditions, most of the $CsNO_3$ derivatives are in CsOH as a chemical form. Thermodynamic calculation suggests that the stability of the promoter at 600 K is in the order of CsOH > Cs > Cs_2O and some metallic form of Cs can exist if no additives are added (4). We once studied the temperature-programmed decomposition of $CsNO_3$ under a hydrogen stream (41), and concluded that the main phase was CsOH on the oxide-supported Ru (41), but the metallic Cs can be alive on the Raney Ru system (47). The state of the cesium promoter may be dependent on the condition (water pressure and temperature) and the state of the catalyst or its ability to form surface hydroxide. In this sense, BaO and CsOH can be compared to zeolite (37) and MgO (29) systems; however, BaO and CsOH/Cs must be compared to a carbon support (24, 34, 38), which can not possibly bear hydroxyls. These kinds of problem should also be solved in the future.

In the case of the $Fe–Al_2O_3–K_2O$ catalyst, only KOH is thought to be a stable species and K_2O, K, and potassium nitride cannot be present under normal ammonia-synthesis conditions (2, 4). If the water concentration is above about 10^{-2} ppm, no appreciable amount of K_2O is present judging from the equilibrium constant of $K_2O + H_2O = 2KOH$.

The electron-donation effect of hydroxides must be lower than the oxides, because the electronegativities of CsOH (1.73) and KOH (1.81) are higher than those of oxides Cs_2O (1.20) and K_2O (1.31) (1, 46). It should be noted that the electronegativities of CsOH and KOH are comparable to that of BaO (1.77), suggesting that BaO acts with a similar electronic promotion effect on ammonia synthesis. In the case of barium, therefore, it is important to keep the promoter in oxide states during ammonia synthesis to complete with alkali promoters.

4.3. *State of BaO and the Interaction with Ru*

The covalent radius of any element (i.e., 0.66 A for O atom) expands when an electron is added (1.40 A for O^{2-}) (46). The ionic or covalent radius is a good measure to estimate the atomic distance. For example, the sum (2.75 A) of the ionic radius of Ba^{2+} (1.35 A) and that of O^{2-} (1.40 A) fit well with the bond distance of BaO (2.77 A) (37, 46). However, the reported bond distance between Ru and O (of promoter or support oxide) is unique. XAFS studies have proposed the short distance of 2.1 A for Ru_3/CeO_2 (48) and 2.1 A for Ru/CsMgO and Ru/KX-zeolite (37) and an even shorter distance of 1.9 A for BaO–Ru/BaX-zeolite (37). If we apply the radius of neutral Ru (1.325 A as the metal or 1.24 A as the covalent form) and anion O^{2-} (1.40 A), the bond distance is given as 2.73 or 2.64 A, which is much longer than the 2.1 or 1.9 A of XAFS data. If the oxygen atom were neutral (0.66 A), it might give 1.99 or 1.90 A. If ruthenium were oxidized, ionic pair of Ru^{3+}(0.77 A) and O^{2-}(1.40 A) would give the atomic distance of 2.17 A. These values look reasonable; however, neutral oxygen or oxidized ruthenium is not acceptable. Oxygen must be a counterpart of the barium cation or support cation. The unusual short distance may come from the nature of isolated cluster atoms. Where the coordination number is low or atoms are surrounded by few atoms, contradiction may occur (48, 37).

BaO might be isolated on the ruthenium surface as has been discussed by Hansen *et al.* (31). Our current study suggests that the nature of (bulk) BaO is preserved at least in the sense of the thermodynamic relation with water and electronegativity discussion. Of course, this discussion was justified from the activity comparison and does not come from absolute calculations. When these compounds are adsorbed and isolated on the surface, every chemical constant could be changed. However, the relative trend may trace the bulk nature. We cannot conclude the state of BaO here; however, it can be accepted that BaO is adsorbed on the Ru surface (31). With regard to the questions in the introduction, category 2, in which the promoter just donates electrons to normal Ru surfaces, which weakens the N–N bond and accelerates dinitrogen dissociation (5–14), or 3, in which the promoter further helps the dissociation at the special site (such as B5 site) by the combination of the structural effect and electronic effect (33), must be true. These problems should be studied further.

5. CONCLUSIONS

The promoter components derived from $Ba(NO_3)_2$ as the promoter precursor on the Ru/AC catalyst were BaO and $Ba(OH)_2$ in mixture, of which the molar ratio varied with (the treatment or the reaction) temperature and water vapor pressure, obeying the reversible reaction $BaO + H_2O = Ba(OH)_2$ with $\Delta H^0_{298} = -34.9$ kcal/mol, in both the catalyst-activation process (hydrogenolysis process) and the ammonia-synthesis process. The active-promoter form is proposed to be BaO rather than $Ba(OH)_2$. The activity changes reversibly with the ratio of BaO to $Ba(OH)_2$. Increasing the treatment temperature and eliminating moisture from synthesis gas increases the BaO component, thereby increasing the activity. Above 648 K (estimated operation temperature in the commercial process), BaO becomes rich under a water vapor pressure of 10 Pa. This means water must be controlled below 10 Pa in the process if 1Ba–5Ru/HTAC is used. K or Cs promoters are considered as hydroxides, which cannot be turned to oxide under usual conditions, judging from the thermodynamic data.

Though high-temperature treatment is beneficial for activating the barium promoter, an extremely high-temperature treatment could simultaneously induce the methanation of carbon support, destroying the catalyst morphology and shortening the life of the catalyst (44).

Oxygen-containing molecules, e.g., H_2O, CO_2, CO, etc., are often strong and irreversible poisons for the Fe catalyst in ammonia synthesis (2). Moisture contained in the synthesis gas decreases the amount of the active-promoter component BaO and hence decreases the catalytic activity; however, it recovers reversibly if water vapor is removed. Ru catalysts are known to be less sensitive than Fe catalysts for CO poisoning in ammonia synthesis. It was concluded in this study that the BaO-promoted Ru/AC catalyst can be activated reversibly after making contact with oxygen-containing molecules.

ACKNOWLEDGMENT

This work was financed by the Ministry of Education, Culture, Sports, Science and Technology of the Japanese Government under grant number 12793002.

REFERENCES

1. Aika, K., and Tamaru, K., *in* "Ammonia: Catalysis and Manufacture" (A. Nielsen, Ed.), Chap. 1–6. Springer-Verlag, Berlin, 1995.
2. Ozaki, A., and Aika, K., *in* "Catalysis—Science and Technology" (J. R. Anderson and M. Boudart, Eds.), Chap. 3, p. 87. Springer-Verlag, Berlin, 1981.
3. Foster, A. I., James, P. G., McCarroll, J. J., and Tennison, S. R., U.S. Patent No. 4,163,775 (1979); Foster, A. I., James, P. G., McCaroll, J. J., and Tennison, S. R., U.S. Patent No. 4,250,057 (1981); McCarroll, J. J., Tennison, S. R., and Wilkinson, N. P., U.S. Patent No. 4,600,571 (1986).
4. Tennison, S., *in* "Catalytic Ammonia Synthesis" (J. R. Jennings, Ed.), pp. 303–364, Plenum, New York, 1991.
5. Van Ommen, J. G., Bolink, W. J., Prasad, J., and Mars, P., *J. Catal.* **38**, 120 (1975).
6. Jacobsen, C. J. H., Dahl, S., Hansen, P. L., Tornqvist, E., Jensen, L., Topsoe, H., Prip, D. V., Moenshaug, P. B., and Chorkendorff, I., *J. Mol. Catal., A* **163**, 19 (2000).
7. Murata, S., and Aika, K., *J. Catal.* **136**, 110 (1992).
8. Murata, S., and Aika, K., *Appl. Catal., A* **82**, 1 (1992).
9. Khaja Masthan, S., Sai Prasad, P. S., Rama Rao, K. S., and Kanta Rao, P., *J. Mol. Catal.* **67**, L1 (1991).
10. Aika, K., and Ozaki, A., *J. Catal.* **13**, 232 (1969).
11. Moggi, P., Albanesi, G., Predieri, G., and Spoto, G., *Appl. Catal., A* **123**, 145 (1995).
12. Aika, K., Kubota, J., Kadowaki, Y., Niwa, Y., and Izumi, Y., *Surf. Sci.* **121–122**, 488 (1997).
13. Kubota, J., and Aika, K., *J. Phys. Chem.* **98**, 11293 (1994).
14. Aika, K., *Catal. Catal.* **40**, 588 (1998).
15. Murata, S., and Aika, K., *J. Catal.* **136**, 118 (1992).
16. Aika, K., Takano, T., and Murata, S., *J. Catal.* **136**, 126 (1992).
17. Kowalczyk, Z., Jodzis, S., Rarog, W., Zielinski, J., and Pielaszek, J., *Appl. Catal., A* **173**, 153 (1998).
18. Rosowski, F., Hornung, A., Hinrichsen, O., Herein, D., Muhler, M., and Ertl, G., *Appl. Catal., A* **151**, 443 (1997).
19. Moggi, P., Albanesi, G., Predieri, G., and Spoto, G., *Appl. Catal., A* **123**, 145 (1995).
20. Rossetti, I., Pernicone, N., and Forni, L., *Appl. Catal., A* **208**, 271 (2001).
21. Forni, L., Molinari, D., Rossetti, I., and Pernicone, N., *Appl. Catal., A* **185**, 269 (1999).
22. McClaine, B. C., Becue, T., Lock, C., and Davis, R. J., *J. Mol. Catal., A* **163**, 105 (2000).
23. Liang, C. H., Wei, Z. B., Xin, Q., and Li, C., *Appl. Catal., A* **208**, 193 (2001).

24. Aika, K., Kawahara, T., Murata, S., and Onishi, T., *Bull. Chem. Soc. Jpn.* **63**, 1221 (1990).
25. Aika, K., Ohya, A., Ozaki, A., Inoue, Y., and Yasumori, I., *J. Catal.* **92**, 305 (1985).
26. Dahl, S., Taylor, P. A., Tornqvist, E., and Chorkendorff, I., *J. Catal.* **178**, 679 (1998); Dahl, S., Tornqvist, E., and Chorkendorff, I., *J. Catal.* **192**, 381 (2000).
27. Strongin, D. R., Bare, S. R., and Somorjai, G. A., *J. Catal.* **103**, 281 (1987).
28. Hinrichsen, O., Rosowski, F., Hornung, A., Muhler, M., and Ertl, G., *J. Catal.* **165**, 33 (1997).
29. Bielawa, H., Hinrichsen, O., Birkner, A., Muhler, M., and Ertl, G., *Angew. Chem., Int. Ed. Engl.* **40**, 1061 (2001).
30. Dahl, S., Sehested, J., Jacobsen, C. J. H., Tornqvist, E., and Chorkendorff, I., *J. Catal.* **192**, 391 (2000).
31. Hansen, T. W., Jacob, B. W., Hansen, P. L., Dahl, S., Topsoe, H., and Jacobsen, C. J. H., *Science* **294**, 1508 (2001); Jacobsen, C. J. H., *J. Catal.* **200**, 1 (2001).
32. Schlögl, R., Wiesendanger, R., and Baiker, A., *J. Catal.* **108**, 237 (1987).
33. Jacobsen, C. J. H., Dahl, S., Hansen, P. L., Törnqvist, E., Jensen, L., Topsøe, H., Prip, D. V., Møenshaug, P. B., and Chorkendorff, I., *J. Mol. Catal. A: Chem.* **163**, 19 (2000).
34. Zhong, Z. H., and Aika, K., *Inorg. Chim. Acta.* **280**, 183 (1998).
35. Kowalczyk, Z., Jodzis, S., Rarog, W., Zielinski, J., Pielaszek, J., and Presz, A., *Appl. Catal., A* **184**, 95 (1999).
36. Zhong, Z. H., and Aika, K., *Chem. Commun.* 1223 (1997).
37. McClaine, B. C., Siporin, S., and Davis, R. J., *J. Phys. Chem. B* **105**, 7525 (2001).
38. Kowalczyk, Z., Jodzis, S., Rarog, W., Zielinski, J., and Pielaszek, J., *Appl. Catal., A* **173**, 153 (1998); Rarog, W., Kowalczyk, Z., Sentek, J., Sklandanowski, D., and Zielinski, J., *Catal. Lett.* **68**, 163 (2000).
39. Chao, K. J., Lin, L. H., and Yang, M. H., *Catal. Lett.* **38**, 279 (1996).
40. Aika, K., Kumasaka, M., Oma, T., Kato, O., Matsuda, H., Watanabe, N., Yamazaki, K., Ozaki, A., and Onishi, T., *Appl. Catal.* **28**, 57 (1986).
41. Aika, K., Shimazaki, K., Hattori, Y., Ohya, A., Ohshima, S., Shirota, K., and Ozaki, A., *J. Catal.* **92**, 296 (1985).
42. Zhong, Z. H., and Aika, K., *Catal. Catal.* **39**, 138 (1997).
43. Zhong, Z. H., and Aika, K., *J. Catal.* **173**, 535 (1998).
44. Zeng, H. S., Inazu, K., and Aika, K., *Appl. Catal., A* **219**, 235 (2001).
45. Cho, S. J., and Kang, S. K., *J. Phys. Chem. B* **104**, 8124 (2000).
46. *In* “Langes Handbook of Chemistry, 11th Edition” (J. A. Dean, Ed.), Chap. 3, p. 118. McGraw–Hill, New York, 1973.
47. Hikita, T., Kadowaki, Y., and Aika, K., *J. Phys. Chem.* **95**, 9396 (1991).
48. Izumi, Y., Iwata, Y., and Aika, K., *J. Phys. Chem.* **100**, 9421 (1996).
49. Cassir, M., Piolet, C., Moneuse, C., and Devynck, J., *Electrochim. Acta.* **34**, 1563 (1989); Konigstein, M., *J. Solid State Chem.* **147**, 478 (1999).